VIBRATION ANALYSIS OF GLASS FIBER REINFORCED COMPOSITES

R. K. Mishra
Department of Mechanical Engineering, Gautam Buddha University, Gautam Buddha nagar, Greater Noida, India

Abstract:
Glass fiber reinforced resol/vac-eha composites have been fabricated in laboratory to determine the dynamic behavior of glass fiber reinforced composites. Resol solution was blended with vinyl acetate-2-ethylhexyl acrylate (vac-eha) resin in an aqueous medium with varying volume fraction of glass fibers. The role of fiber/matrix interactions in glass fibers reinforced composites were investigated to predict the stiffness and damping properties. In order to study the static and dynamic response of Resol, Resol/VAC-EHA blend and glass fibers reinforced composites, a multiquadric radial basis function (MQRBF) method is developed. MQRBF is applied for spatial discretization and a Newmark implicit scheme is used for temporal discretization. The discretization of the differential equations generates a larger number of algebraic equations than the unknown coefficients. To overcome this ill conditioning, the multiple linear regression analysis, which is based on the least square error norm, is employed to obtain the coefficients. Simple supported and clamped boundary conditions are considered. Numerical results are compared with those obtained by other analytical methods.

Notations : a, b -Dimension of plates, h ----Thickness of plates, R ----Aspect ratio (a/b), ν_{LT} --- Major Poisson's ratio, C_ν^*, C_ν ----Viscous damping, dimensionless viscous damping, $D_{11}, D_{22}, D_{12}, D_{66}$ ----Flexural rigidity of plates, E_L, E_T ----Young's modulus in x^*, y^* direction respectively, G_{LT} ---Shear modulus relative to x^*-y^* direction, q, Q ---Transverse load, dimensionless transverse load, t^*, t ---Time, dimensionless time, w^* ----Displacement in z^* direction, w ---Dimensionless displacement in z direction

Key words: *Glass fiber, Resol, vinyl acetate-2-ethylhexyl acrylate, multiquadric radial basis function glass fiber-reinforced composites.*

Introduction:

Fiber-reinforced composites based upon thermoplastic polymer matrices and thermoplastic-thermoset interpenetrating network (IPN) polymer matrices potentially offer several advantages compared to those based upon thermosetting resin matrices. The early 1980s thermosetting matrix composites were used in significant positions of the primary structure of military aircraft and secondary structure of commercial aircraft. Composites are used because of their weight savings compared with metals, and hence reduced fuel consumption, longer-range, higher performance or greater payload. It was recognized that thermoset composites were sensitive to damage, and in particular to low energy and low velocity impacts, which occur in routine service. Thermoset Phenolic resin is one of the earliest synthetic resins to possess excellent fire retardancy, low smoke density and toxic emission [1-3], though its application is limited because unmodified phenolic is a brittle material. A lot of research work has been conducted to toughen phenolic resin. The polyester-phenolic copolymer has been synthesized to improve the mechanical properties and heat resistance [4] the flexural strength improves when phenoxy resin is blended with resol-type phenolic resin [5]. Various types of fibers are used for reinforcement; these are glass fibers, carbon fibers and polyethylene fibers etc. but glass fiber-reinforced composites are used extensively in various applications. Glass fibers have high mechanical and bending properties. Mechanical properties of the fiber reinforced composites are different from mechanical properties of the fibers [6-7]. It depends upon various factors. These are fiber orientation, weight and volume fraction of the fibers and matrix, bonding between fibers and matrix. To predict the static and dynamic behavior of the composite is very important when it is used in structural applications. The static and dynamic behavior of the unidirectional banana fibers reinforced high-density polyethylene/ poly (Є-caprolactone) composites have been presented by Misra et al [8] Normally finite element method is used to predict the behavior of composites. But in finite element method generation of mesh is tedious and time-consuming task. To avoid this problem meshless methods have been developed. In various meshless methods importance of the multiquadric radial basis function method (MQRBF) is increasing day by day. In1971, it was proposed by Hardy [9] for the interpolation of geographically scattered data. Franke [10] has ranked MQRBF is the best interpolation method based on its accuracy, visual aspect, sensitivity to parameters, execution time and ease of implementation. Later on this method was used by Kansa [11] to solve partial differential equations. Ferreira applied the radial basis function for the analysis of composite beams [12] and plates [13]. Misra et al [14-15] used this method for the analysis of anisotropic plates and laminate. The properties of the resol improve by blending vinyl acetate-2-ethylhexyl acrylate copolymer (VAC-EHA) by IPN technique. This paper reports fabrication and evaluation of the mechanical properties of glass fibers reinforced Resol/VAC-EHA composites at different volume fraction of the fibers. After obtaining the properties experimentally, MQRBF method is employed for static and dynamic analysis of unidirectional glass fibers reinforced Resol/VAC-EHA composite plate.

Experimental Studies:

- **Materials**

❖ Resol was prepared by the method cited in the literature [16-17].
❖ The hardener for resol was para-toluene sulphonic acid (PTSA), 0982 H from Bakelite AG.
❖ VAC-EHA copolymer in emulsion form was obtained from macromoles, India.
❖ Hydroxy methoxy methyl melamine (HMMM) was prepared in the laboratory using standard procedure [18].
❖ Glass Fiber (433 BF-225) supplied by Indian Petrochemicals Corporation Ltd., Boroda, India.

Preparation of Composites:
The individual polymers were first separately diluted with distilled water to maintain a solid content of 50 % by weight for convenience, under well-stirred condition. Then a weighed amount of resol was taken in a three-necked round bottom flask. VAc-EHA copolymer was then accurately weighed into the flask and the contents were stirred to give a homogeneous mixture in the desired blend ratio of the components. Para-toluene sulfonic acid (PTSA) 7 % by weight based on resol was thoroughly mixed for 20 minutes [19]. Then hydroxy methoxy methyl melamine (HMMM) was added at 20 % by weight of VAc-EHA copolymer. The prepeg of glass fiber was prepared previously. For the use of treated fiber in making composites, the fibers were treated with chromic acid at room temperature for 15 min. When the formation of the bubbles ceased, the viscous mass was poured into a glass mold prepared by clipping together two glass plates separated by a Teflon gasket in between, the thickness of which controls the thickness of the sample sheet formed. It was then initially kept at room temperature for about 24 hours and then heated at 80^0 C for 4 hours [20]. Thus, the samples were produced.

- **Tensile Properties:**

An Instron universal – testing machine (Model 3360) was used for measuring the mechanical properties like tensile strength and tensile modulus. ASTM D638 method was followed. A crosshead speed of 5 mm/min was maintained. All testing were conducted under ambient conditions in an environmentally controlled room. The data reported are averages of at least six measurements, and typical scattering range of the results was ±5 %.

Theoretical Analysis:
After evaluating the mechanical properties of the unidirectional glass fibers reinforced Resol/VAC-EHA composites at different volume fraction of the fibers, Multiquadric radial basis function method is applied for static and dynamic analyses of the unidirectional glass fibers reinforced Resol/VAC-EHA composite plate to assess its response to external loading such as uniformly distributed load.

- **The Multiquadric Radial Basis Function Method**

Consider a general differential equation

$$Aw = f(x, y) \quad \text{in} \quad \Omega \tag{1}$$

$$Bw = g(x, y) \quad \text{on} \quad \partial\Omega \tag{2}$$

where A is a linear differential operator and B is a linear boundary operator imposed on boundary conditions for the orthotropic plate. In the present research work, it is assumed that the glass fiber reinforced composite plate behaves as an orthotropic plate since the diameter of glass fiber is so small that its contribution to the strength is predominantly along its longitudinal direction only.

Let $\{P_i = (x_i\ ,\ y_i)\}_{i=1}^{N}$ be *N* collocation points in domain Ω of which $\{(x_i\ ,\ y_i)\}_{i=1}^{N_I}$ are interior points; $\{(x_i\ ,\ y_i)\}_{i=N_I+1}^{N}$ are boundary points. In MQRBF method, the approximate solution for differential equation (1) and boundary conditions (2) can be expressed as:

$$w(x, y) = \sum_{j=1}^{N} w_j \varphi_j(x, y) \tag{3}$$

and multiquadric radial basis as:

$$\varphi_j = \sqrt{(x - x_j)^2 + (y - y_j)^2 + c^2} = \sqrt{r_j^2 + c^2} \tag{4}$$

where $\{w_j\}_{j=1}^{N}$ are the unknown coefficients to be determined, and $\varphi_j(x_j, y_j)$ is a basis function. Other widely used radial basis functions are:

$\varphi(r) = (c^2 + r^2)^{1/2}$ Multiquadrics

$\varphi(r) = (c^2 + r^2)^{-1/2}$ Inverse multiquadrics

$\varphi(r) = r^3$ Cubic

$\varphi(r) = r^2 \log(r)$ Thin plate splines

$\varphi(r) = (1-r)^m_+ p(r)$ Wendland functions

$\varphi(r) = e^{-(cr)^2}$ Gaussian

Here c is a shape parameter, a positive constant. Ling and Kansa [21] discussed about the shape parameter.

Results and Discussion:

Figure 1 shows the theoretical and experimental Young's modulus of the glass fiber reinforced composites in longitudinal direction at different volume fraction of the fibers. Young's modulus (E_L) appears to be linearly dependent on volume fraction of the fibers (V_f). As soon as volume fraction of the fiber increases theoretical and experimental Young's modulus increases, but theoretical Young's modulus increases at higher rate as compared to experimental Young's modulus.

The interesting feature of this study is that the distance between corresponding theoretical and experimental curves increases with V_f, and the deviation is minimum at lower range of V_f . In the present work, the hand lay-up technique has been used with a V_f range of 0.089-0.357. At a higher V_f, fiber interaction takes place, and either they tend to bundle up among themselves or they touch each other physically, which is due to the fact that hand lay-up technique produces more or less random nature of fiber distribution in the matrix. Due to the above facts, proper and uniform penetration of the matrix does not take place throughout the fiber surfaces, leaving interstitial voids. Thus, the degree of fiber misalignment and void content increases with the increase in V_f. These facts are reflected in the experiment by the deviation of the experimental curve from the theoretical one. Longitudinal and transverse Young's modulus of the glass fiber reinforced composites at different volume fraction of the fibers has been shown in figure 2. When volume fraction of the fibers is 8.8 % difference between both Young's modulus is less but as soon as volume fraction of the fiber increases difference between both Young's modulus also increases. Figure 3 shows the stress- strain behavior of the glass fiber reinforced composites and the Resol/VAC-EHA matrix. The failure strain of glass fiber is about 2 times than the matrix (ε_m). The stress- strain curve display a point of inflection (Knee point) around ε_m , which enables the curve to be approximated by two regions – one indicating the elastic (below the point corresponding to ε_m) , other the plastic region (beyond the point corresponding to ε_m). It is established that the elastic region of the composite is dependent on ε_m. The increase in fiber content leads to an increase in the first crack stress (corresponding to ε_m), and the ultimate strain. It is observed from the stress-strain curves that the main influence of the fibers is in the post-cracking zone, where the contribution of the matrix is small or even negligible.

The experimental and theoretical tensile strength of the glass fiber reinforced composites has been compared and shown in figure 4 at different volume fraction of the fibers. From the graph it is established that the elastic region of the composite is dependent on matrix. The increase in fiber content leads to an increase plastic deformation. The experimental tensile strength is less than theoretical tensile strength. Figure 5 shows the elongation at break of the glass fiber reinforced composites at different volume fraction of the fibers. It is observed that elongation shows linear relationship upto 17.6 % volume fraction of the fibers but becomes constant from 17.6 % to 25.4 % volume fraction of fibers and after 25.4 % volume fraction of fibers it increases slowly. Table 1 shows the tensile modulus of the Resol and Resol/VAC-EHA blends. Tensile modulus decreases due to increase blending of VAC-EHA copolymer content in Resol. The mechanical properties of the glass fiber reinforced Resol/VAC-EHA composites are studied to observe the effect of glass fiber by increasing its volume fraction has been shown in Table 2. As volume fraction of fiber increases from 8.8 % upto 35.3 %, longitudinal modulus of elasticity increases 53.75 %, 96.40 % and 142.42% respectively.

Case Study: Static and Dynamic Response of the Composite plate

Figure 6 shows the geometry, coordinate system and loading in glass fiber reinforced composites. Neglecting the transverse shear and rotary inertia, equation of glass fiber reinforced composites is expressed in non-dimensional form as:

$$(w_{xxxx} + 2R^2\eta w_{xxyy} + R^4\psi w_{yyyy}) + w_{tt} + c_v w_t - Q(x,y,t) = 0 \quad (5)$$

where the subscript denotes the partial derivative with respect to the suffix following. The non-dimensional quantities are defined by

$$w = w^*/h, x = x^*/a, y = y^*/b, R = a/b, t = t^*\sqrt{D_{11}/(\rho a^4 h)}$$

$$Q = qa^4/(D_{11}h), C_v = (C_v^*/M)\sqrt{(\rho a^4 h)/D_{11}}, M = \rho abh$$

$$\eta = (D_{12} + 2D_{66})/D_{11}, \psi = D_{22}/D_{11} \quad (6)$$

Boundary conditions for the plate simply supported at all four edges are:

$x = 0,1 \qquad w = 0$ (7a)

$x = 0,1 \qquad w_{xx} = 0$ (7b)

$y = 0,1 \qquad w = 0$ (7c)

$y = 0,1 \qquad w_{xx} = 0$ (7d)

Boundary conditions for the clamped edge plate are:

$x = 0,1 \qquad w = 0$ (8a)

$x = 0,1 \qquad w_x = 0$ (8b)

$y = 0,1 \qquad w = 0$ (8c)

$y = 0,1 \qquad w_y = 0$ (8d)

The governing equation (5) is solved using multiquadric radial basis function and boundary conditions, equations (7) and (8), for simply supported and clamped edge plates respectively, and has been presented in Appendix A. In this multiquadric radial basis function method number of algebraic equations creates more than the number of unknown coefficients $\{w_j\}_{j=1}^{N}$. Hence this method creates ill conditioning. To overcome this ill-conditioning, multiple linear regressions analysis (Appendix B) based on least-square error norms is employed. Deflection of the pure Resol, Resol/VAC-EHA blends and glass fiber reinforced composite plate at various aspect ratios of the present method for simply supported boundary condition has been compared with those obtained by Timoshenko and Woinowsky-Krieger [22] and Whitney [23] as shown in Tables [3-11]. There is good agreement between the present results and reference solution. The following features are observed after analyzing the Tables 3-11 for simple supported boundary conditions:

- As aspect ratio increases deflection decreases due to decrease in load.
- Resol/VAC-EHA (F20) blends Plate gives maximum deflection and 35.3 % glass fiber reinforced composite plate gives least deflection. It means strength of the Resol/VAC-EHA (F20) blends plate is least and 35.3 % glass fiber reinforced composite plate is maximum.

- As percentage of the VAC-EHA copolymer increases deflection also increases and strength decreases.

Similar behavior is observed at clamped edge boundary conditions as shown in Table 12 and 13, but clamped edge plate deflect less as compared to simple supported plate. A computer program based on the finite difference method (FDM) proposed by Chadrashekara [24] (Chadrashekara, 2001) is also developed. The damped response of the simple supported composite plates obtained by the present method and finite difference method has been compared and shown in Figure 7 at uniformly distributed load q = 10 (N/m^2), sides a = b = 300 (mm) and thickness h = 10 (mm) at non-dimensional viscous damping factor C_v = 1.25. There is good agreement in the results. The following features are observed after analyzing Figures 8-14 for the simple supported boundary condition:

- Resol/VAC-EHA blends plate takes more time to stabilize as compared to pure Resol and 8.8 % glass fiber reinforced composite plate.

- As soon as percentage of the glass fiber increases from 8.8 % upto 35.3 % damping property of the composite plate increases.

- At same volume fraction, aspect ratio (b/a) of the glass fiber reinforced composite plate increases stability time also increases.

After incorporation of glass fibers in composite materials, tensile properties, tensile modulus, stiffness and damping properties increase. Damping means capacity of the materials to dissipate energy. Here glass fibers dissipate more energy as compared to Resol/VAC-EHA matrix**.**

Similar behavior is observed at clamped edge boundary conditions as shown in Figure 15 , but clamped edge plate takes more time to stabilize as compared to simple supported plate because clamped edge plate dissipate less energy.

Conclusion:

Glass fiber reinforced Resol/VAC-EHA composites plate has been prepared in laboratory to evaluate the mechanical properties. Damping properties decrease after blending VAC-EHA copolymer content with Resol. Tremendous changes occur in mechanical properties when glass fibers are reinforced with Resol/VAC-EHA blends. Resol, Resol/VAC-EHA blends and glass fibers reinforced composite plate show different mechanical response at static and dynamic loading. As soon as quantity of the glass fibers increase in composite plate damping properties increase. Due to incorporation of glass fibers in matrix, tensile properties, stiffness and damping properties increase. It has been found that MQRBF method is most suitable to predict the mechanical behavior of composite plate at static and dynamic loading.

Appendix

A. Multiquadric radial basis function method for governing differential equation

Substitution of multiquadric radial basis function in equation (5) gives

$$(\sum_{j=1}^{N} w_j \frac{\partial^4}{\partial x^4}\varphi_j + 2R^2\eta\sum_{j=1}^{N} w_j \frac{\partial^4}{\partial x^2 y^2}\varphi_j + \sum_{j=1}^{n} R^4\psi w_j \frac{\partial^4}{\partial y^4}\varphi_j) + \sum_{j=1}^{N} w_j \frac{\partial^2}{\partial t^2}\varphi_j + C_v w_j \frac{\partial}{\partial t}\varphi_j - Q = 0 \quad (9)$$

Substitution of multiquadric radial basis function in boundary conditions

For Simple supported edge

$$x = 0, a \qquad \sum_{j=1}^{N} w_j\varphi_j = 0 \quad (10a)$$

$$y = 0, b \qquad \sum_{j=1}^{N} w_j\varphi_j = 0 \quad (10b)$$

$$x = 0, a \qquad \sum_{j=1}^{N} w_j \frac{\partial^2}{\partial x^2}\varphi_j = 0 \quad (10c)$$

$$y = 0, b \qquad \sum_{j=1}^{N} w_j \frac{\partial^2}{\partial y^2}\varphi_j = 0 \quad (10d)$$

For clamped edge

$$x = 0, a \qquad \sum_{j=1}^{N} w_j\varphi_j = 0 \quad (11a)$$

$$y = 0, b \qquad \sum_{j=1}^{N} w_j\varphi_j = 0 \quad (11b)$$

$$x = 0, a \qquad \sum_{j=1}^{N} w_j \frac{\partial}{\partial x}\varphi_j = 0 \quad (11c)$$

$$y = 0, b \qquad \sum_{j=1}^{N} w_j \frac{\partial}{\partial y}\varphi_j = 0 \quad (11d)$$

B. Multiple regression analysis

$A.a = p$; Where A = (*l*k)* coefficient matrix, a = (k*1) vector and *p = (l*1)* load vector

Approximating the solution by introducing the error vector e, we get $p = Aa + e$

where e = *(l*1)* vector

To minimize the error norm, let us define a function S as

$$S(a) = e^T e = (p - Aa)^T (p - Aa)$$

The least-square norm must satisfy

$$(\partial S / \partial a)_a = -2A^T p + 2A^T Aa = 0$$

This can be expressed as

$$a = (A^T A)^{-1} A^T P \ or \quad a = B.P$$

The matrix B is evaluated once and stored for subsequent usages.

References:

1. Sperling, L.H. (1981), “Interpenetrating Polymeric Networks and Related Material”, Plenum Press, New York, USA.
2. Frisch, H.L., Frisch, K.C. and Klempner, D. (1981), “Advances in Interpenetrating Polymer Networks”, Pure and Applied Chemistry, 53, 1557-1566.
3. Zaks, Y., Lo, J., Raucher, D. Pearce, E.M. (1982), “Some structure-property relationships in polymer flammability: Studies of phenolic-derived polymers”, J. Appl. Polym. Sci., 27, 913-930.
4. Gardziella, A. and Miller, F.O. (1990), "Environmental importance of phenolic resins and six functions in applications," Kunststoffe, 4, 510-514.
5. Freilich, M.A., Meiers, J.C., Duncan, J.P. and Goldberg, A.J. (2000), “Fiber-reinforced Composites, Quintessence Publishing”, Hong Kong, China, 9 – 21.
6. Herrera-Franco, P.J. and Valadez-Gonza´lez, A. (2005), “A study of the mechanical properties of short natural-fiber reinforced composites”, Composite Part B, 36, 597–608.
7. Ellakwa, A.E., Shorthall, A.C., Shehata, M.K., Marquis, P.M. (2001), “Influence of veneering composite composition on the efficacy of fiber-reinforced restorations (FRR)”, Oper. Dent, 26 (5), 467– 475.

8. Misra, R.K., Sandeep, K., Kumar, S., Misra, A. (2008), "Dynamic Analysis of Banana Fibers reinforced high-density Polyethylene/ Poly (Є-caprolactone) Composites", J. Mech. Mater. Struct, 3(1), 107-126.
9. Hardy, R.L. (1971), "Multiquadric equations of topography and other irregular surfaces", Geophys. Res., 176, 1905–1915.
10. Franke, R. (1982), "Scattered data interpolation: tests of some methods", Math. Comput, 48, 181–200.
11. Kansa, E.J. (1990), "Multiquadrics—a scattered data approximation scheme with applications to computational fluid dynamics: II. Solutions to parabolic, hyperbolic and elliptic partial differential equations", Comput. Math. Appl., 19(8–9), 147–161.
12. Ferreira, A.J.M. (2003), "Thick composite beam analysis using a global meshless approximation based on radial basis functions", Mech. Adv. Mater. Struct, 10, 271–284.
13. Ferreira, A.J.M. (2003), "A formulation of the multiquadric radial basis function method for the analysis of laminated composite plates", Comput. Struct, 59, 385–392.
14. Misra, R.K., Sandeep, K., Misra, A. (2007), "Analysis of anisotropic plate using multiquadric radial basis functions", Int. J. Eng. Anal. Bound. Element, 31, 28-34.
15. Misra, R.K., Sandeep, K., Misra, A. (2007), "Analysis of Cross-ply Laminate using Multiquadric Radial Basis Function", Int. J. Comput. Meth. Eng. Sci. Mech., 8, 1–10.
16. Steiner, P. R. (1975), "Phenol-formaldehyde wood adhesive characterization by proton magnetic resonance spectroscopy", J. Appl. Polym. Sci, 19(1), 215-225.
17. Rudin, A., Fyfe, C.A., Vines, S.M. (1983), "Gel permeation chromatographic analyses of resole phenolic resins", J. Appl. Polym. Sci., 28(8), 2611-2622.
18. Melter, Y.L. (1981), "Water Soluble Polymers Development", since 1978, Noyes Data Corpotion, Park ridge, NJ.
19. Wolfrum, J., Ehrenstein, G.W. (1999), "Interdependence between the curing, structure and the mechanical properties of phenolic resins", J. Appl. Polymer Science, 74(13), 3173-3185.
20. Datta, C., Basu, D., Banerjee, A. (2002), "Studies and Characterization of RESOL/Vac-EHA/HMMM IPN systems in aqueous medium", J. Appl. Polym. Sci., 86(14), 3581-3588.
21. Ling, L., Kansa, E.J. (2004), "Preconditioning for radial basis functions with domain decomposition methods", Math. Comput. Modell, 40, 1413-1427.
22. Timoshenko, S.P., Woinowsky-Krieger, S. (1989), "Theory of plates and shells", II Edition, McGraw-Hill, Kogakusha Ltd, Tokyo.
23. Whitney, J.M. (1987), "Structural analysis of laminated anisotropic plates", Technomic Publishing Company Inc, Lancaster, Pennsylvania, USA.
24. Chandrashekhara, K. (2001), "Theory of plates", Universities Press (India) Limited: Hyderabad, India.

Figure

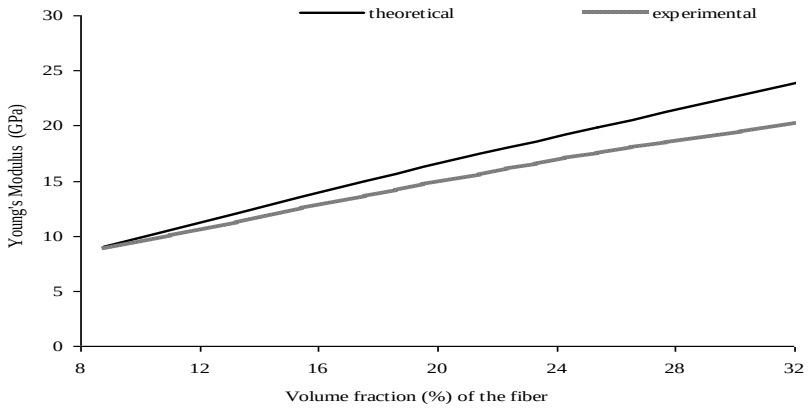

Figure 1: **Theoretical and experimental Young's modulus of the glass fiber reinforced composites in longitudinal direction at different volume fraction of the fibers.**

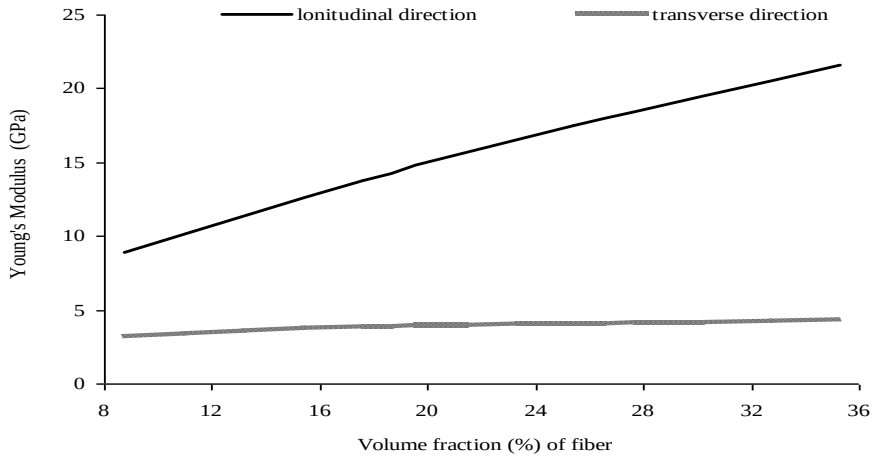

Figure 2: Young's modulus of the glass fiber reinforced composites in longitudinal and transverse direction at different volume fraction of the fibers.

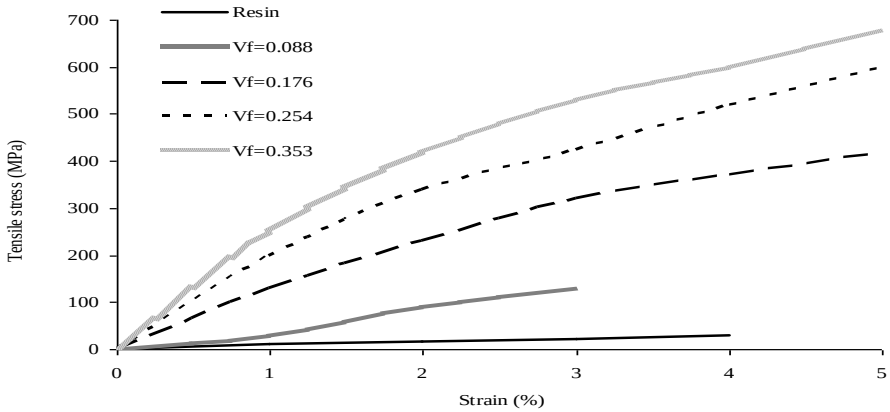

Figure 3: Stress- strain behavior of the glass fiber reinforced composites and the Resol/VAC-EHA matrix.

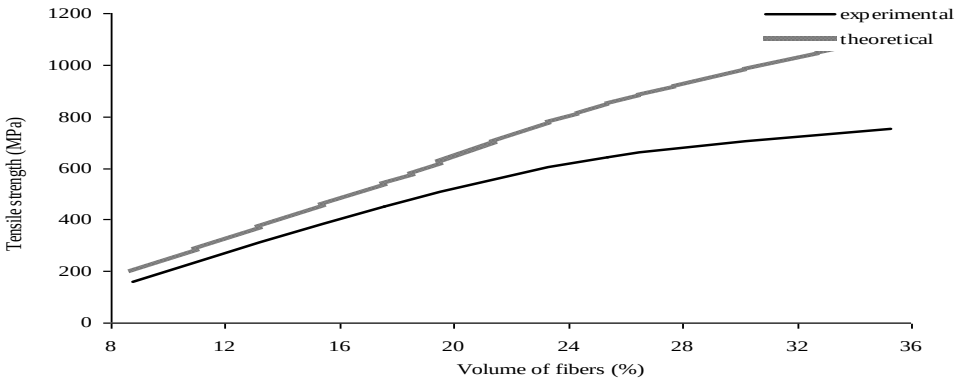

Figure 4: Experimental and theoretical tensile strength of the glass fiber reinforced composites at different volume fraction of the fibers.

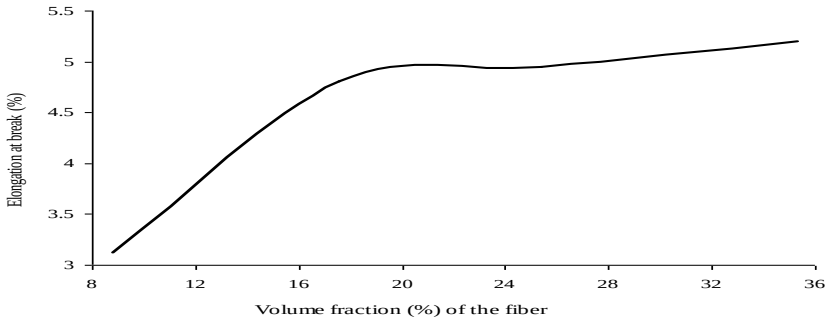

Figure 5: Elongation at break of the glass fiber reinforced composites at different volume fraction of the fibers.

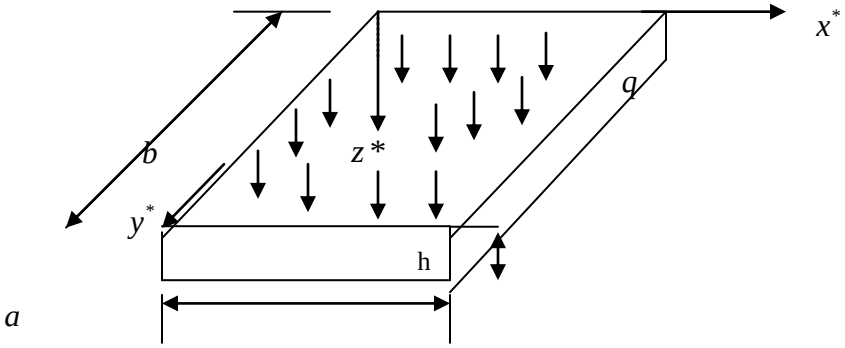

Figures 6: Geometry of the glass fiber reinforced Resol/VAC-EHA blend Composite plate

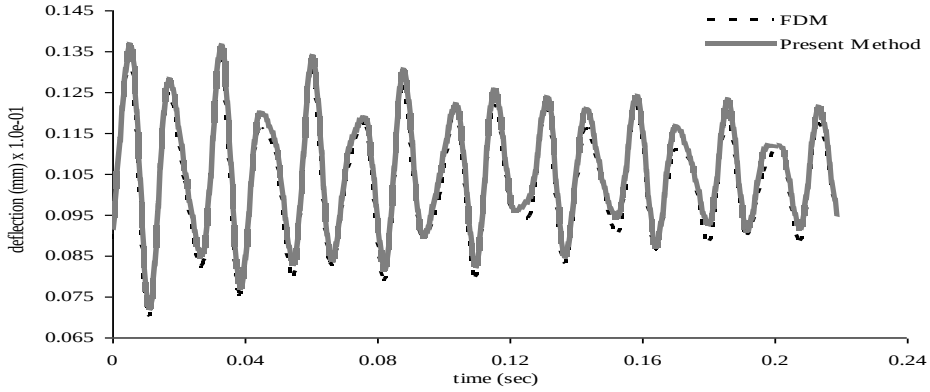

Figure 7: Damped response of a simple supported pure resol square isotropic plate at damping coefficient factor C_v =1.25.

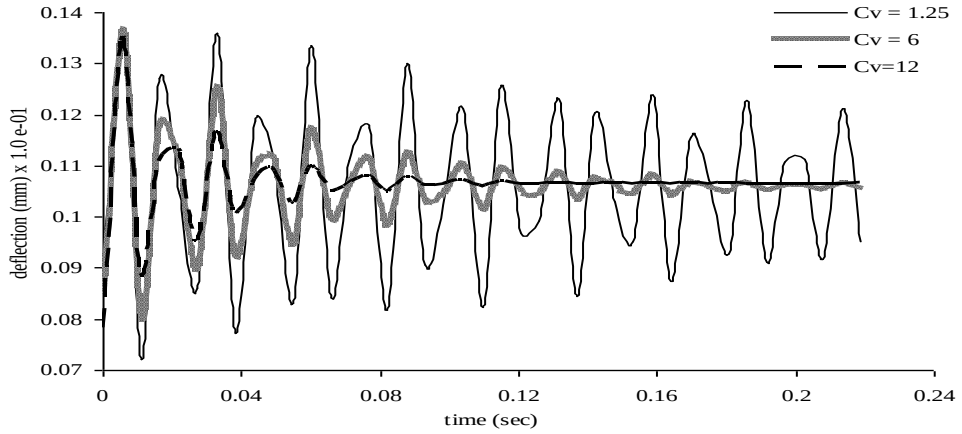

Figure 8: Damped response of a simple supported pure resol square isotropic plate at various damping coefficient factor.

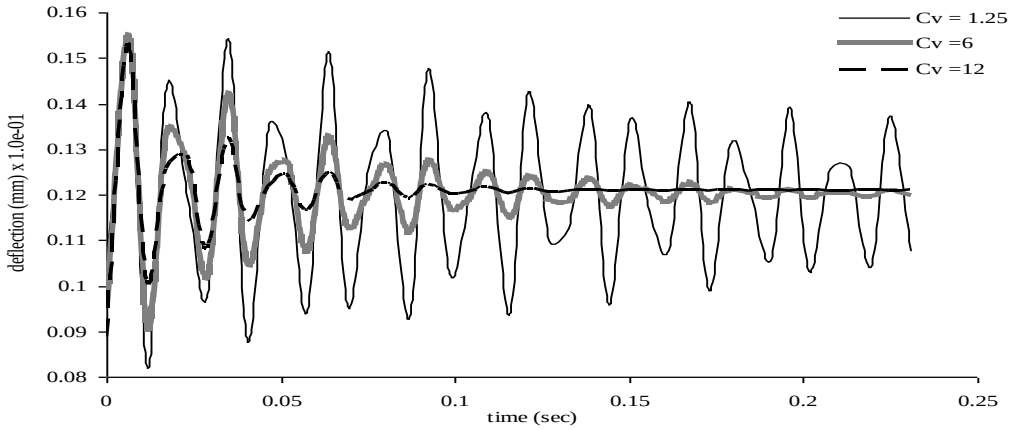

Figure 9: Damped response of a simple supported Resol/VAC-EHA (F20) blends plate at various damping coefficient factor.

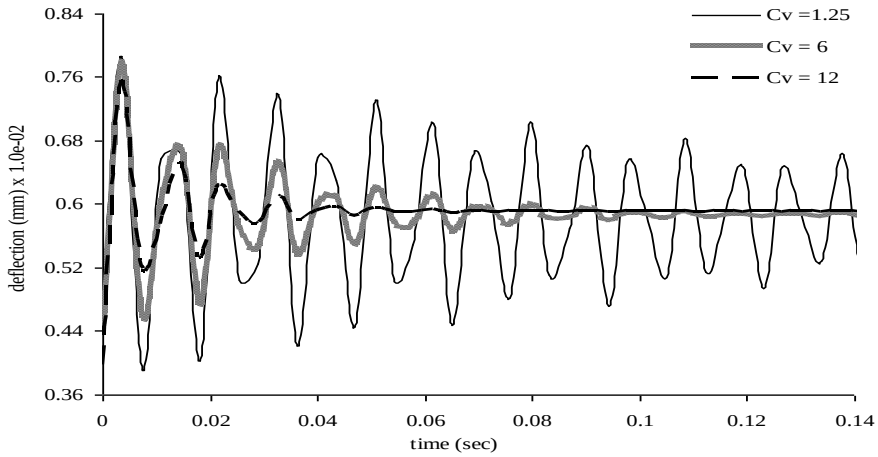

Figure 10: Damped response of a simple supported 8.8% glass fiber reinforced (F20GF8.8) Resol/VAC-EHA blends square composite plate.

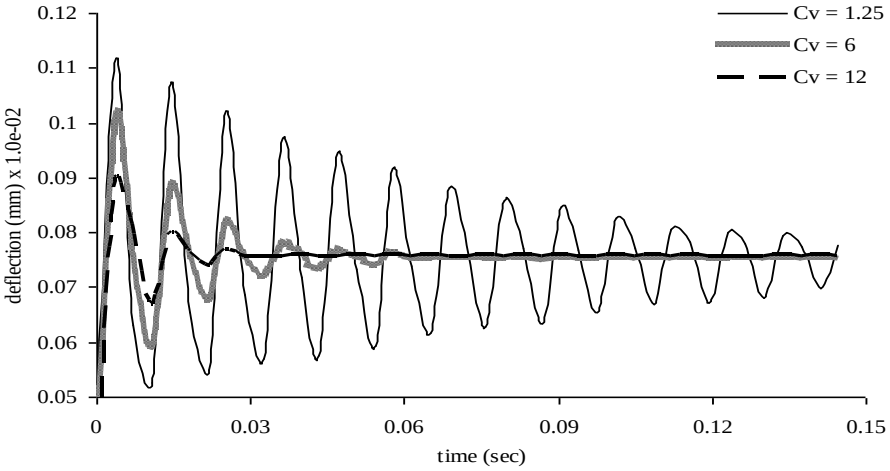

Figure 11: Damped response of a simple supported 8.8% glass fiber reinforced (F20GF8.8) Resol/VAC-EHA blends composite plate at aspect ratio b/a = 2.0

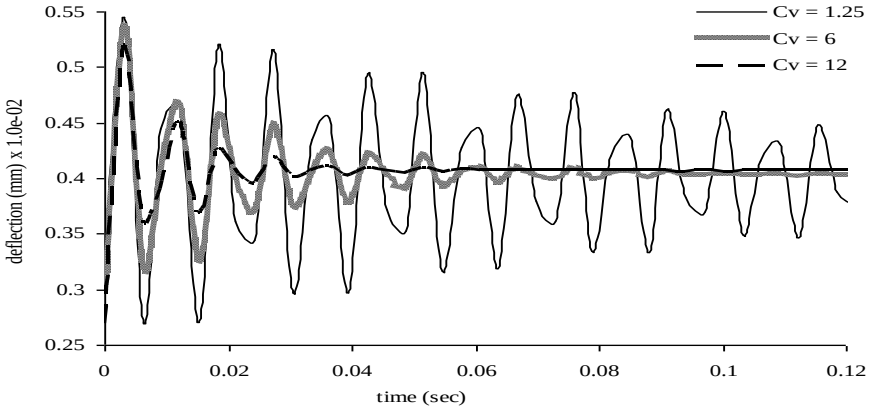

Figure 12: Damped response of a simple supported 17.6 % glass fiber reinforced (F20GF17.6) Resol/VAC-EHA blends square composite plate.

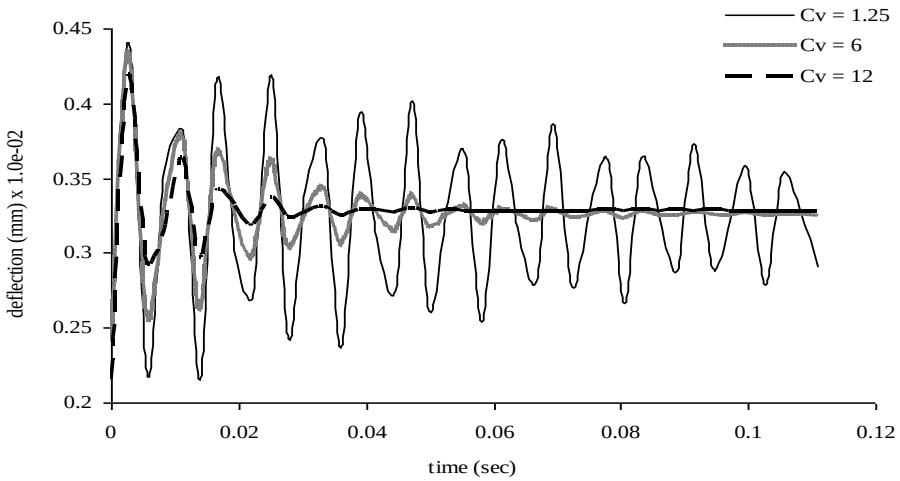

Figure 13: Damped response of a simple supported 25.4 % glass fiber reinforced (F20GF25.4) Resol/VAC-EHA blends square composite plate.

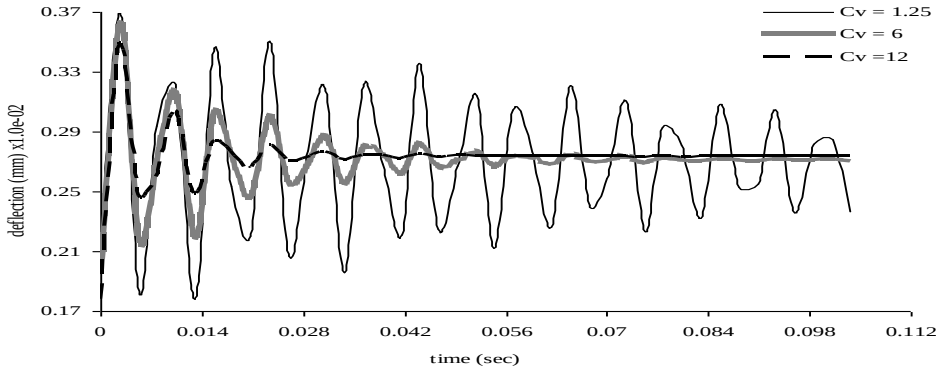

Figure 14: Damped response of a simple supported 35.3 % glass fiber reinforced (F20GF35.3) Resol/VAC-EHA blends square composite plate.

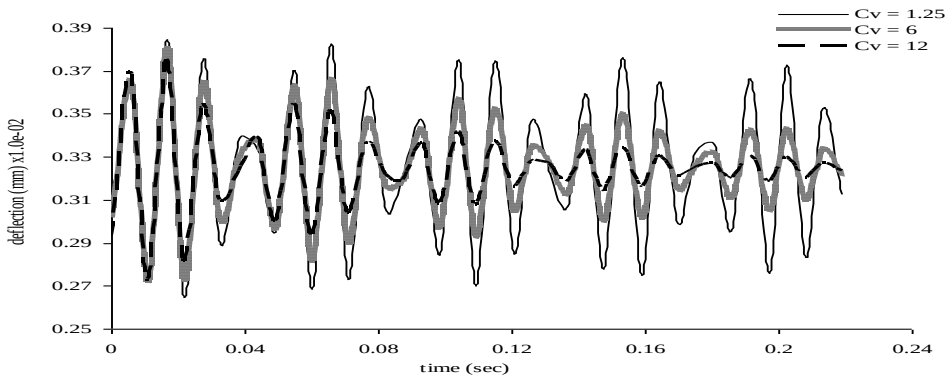

Figure 15: Damped response of a clamped supported pure resol square isotropic plate at various damping coefficient factor.

Table

Table No.1: Tensile modulus of the Resol and Resol/VAC-EHA blends

Code	Materials		Tensile Modulus (GPa)
	Resol % by weight	VAC-EHA % by weight	
Resol	100 %	Nil	3.46
F5	95%	5%	3.25
F10	90%	10%	3.21
F15	85%	15%	3.17
F20	80%	20%	3.05

Table No.2: Mechanical properties of the Glass fibers reinforced in Resol/VAC-EHA (F20) Composites

Code	Volume fraction of fiber in (%)	E_L (GPa)	E_T (GPa)	% Elongation at break
F20GF8.8	8.8	8.91	3.27	3.12
F20GF17.6	17.6	13.7	3.88	4.8
F20GF25.4	25.4	17.5	4.13	4.95
F20GF35.3	35.3	21.6	4.37	5.2

Table No.3: Deflection of the simple supported Resol Plate

q (N/m^2)	b (mm)	a (mm)	b/a	h (mm)	Timoshenko [22] w_{max} (mm)	MQRBF Method w_{max} (mm)
10	300	300	1.0	10	0.0011329	0.0011440
10	300	150	2.0	10	0.00017666	0.00017614
10	300	100	3.0	10	0.000042130	0.000042027

Table No.4: Deflection of the simple supported Resol/VAC-EHA (F5) blends Plate

q (N/m^2)	b (mm)	a (mm)	b/a	h (mm)	Timoshenko [22] w_{max} (mm)	MQRBF Method w_{max} (mm)
10	300	300	1.0	10	0.0010379	0.0010481
10	300	150	2.0	10	0.00016185	0.00016137
10	300	100	3.0	10	0.000038599	0.000038504

Table No.5: Deflection of the simple supported Resol/VAC-EHA (F10) blends Plate

q (N/m^2)	b (mm)	a (mm)	b/a	h (mm)	Timoshenko [22] w_{max} (mm)	MQRBF Method w_{max} (mm)
10	300	300	1.0	10	0.0011050	0.0011159
10	300	150	2.0	10	0.00017231	0.00017180
10	300	100	3.0	10	0.000041093	0.000040992

Table No.6: Deflection of the simple supported Resol/VAC-EHA (F15) blends Plate

q (N/m^2)	b (mm)	a (mm)	b/a	h (mm)	Whitney [23], m= 1,n =1, w_{max} (mm)	MQRBF Method w_{max} (mm)
10	300	300	1.0	10	3.9093e-004	3.945e-004
10	300	150	2.0	10	5.0269e-005	4.903e-005
10	300	100	3.0	10	1.1984e-005	1.168e-005

Table No.7: Deflection of the simple supported Resol/VAC-EHA (F20) blends Plate

q (N/m^2)	b (mm)	a (mm)	b/a	h (mm)	Timoshenko [22] w_{max} (mm)	MQRBF Method w_{max} (mm)
10	300	300	1.0	10	0.0011774	0.0011890
10	300	150	2.0	10	0.00018361	0.00018307
10	300	100	3.0	10	0.000043787	0.000043680

Table No.8: Deflection of the simple supported Glass fibers reinforced Resol/VAC-EHA Composite plate at 8.8% volume fraction of the fibers

q (N/m^2)	b (mm)	a (mm)	b/a	h (mm)	Timoshenko [22] w_{max} (mm)	MQRBF Method w_{max} (mm)
10	300	300	1.0	10	0.0011187	0.0011298
10	300	150	2.0	10	0.00017446	0.00017394
10	300	100	3.0	10	0.000041605	0.000041503

Table No.9: Deflection of the simple supported Glass fibers reinforced Resol/VAC-EHA Composite plate at 17.6 % volume fraction of the fibers

q (N/m^2)	b (mm)	a (mm)	b/a	h (mm)	Whitney [23]m= 1,n =1, w_{max} (mm)	MQRBF Method w_{max} (mm)
10	300	300	1.0	10	5.7270e-004	5.741e-004
10	300	150	2.0	10	7.5908e-005	7.420e-005
10	300	100	3.0	10	1.8203e-005	1.781e-005

Table No.10: Deflection of the simple supported Glass fibers reinforced Resol/VAC-EHA Composite plate at 25.4 % volume fraction of the fibers

q (N/m^2)	b (mm)	a (mm)	b/a	h (mm)	Whitney [23] m= 1,n =1, w_{max} (mm)	MQRBF Method w_{max} (mm)
10	300	300	1.0	10	2.6023e-004	2.648e-004
10	300	150	2.0	10	3.2448e-005	3.158e-005
10	300	100	3.0	10	7.6914e-006	7.472e-006

Table No.11: Deflection of the simple supported Glass fibers reinforced Resol/VAC-EHA Composite plate at 35.3 % volume fraction of the fibers

q (N/m^2)	b(mm)	a(mm)	b/a	h(mm)	Whitney [23]m= 1,n =1 w_{max} (mm)	MQRBF Method w_{max} (mm)
10	300	300	1.0	10	3.1475e-004	3.177e-004
10	300	150	2.0	10	3.9759e-005	3.872e-005
10	300	100	3.0	10	9.4471e-006	9.190e-006

Table No.12: Deflection of clamped edge Resol, Resol/VAC-EHA blends plate

q = 10 (N/m^2) a = b = 300 (mm) h = 10 (mm)	Sample Code	Whitney [23]	MQRBF Method w_{max} (mm)
	F20GF8.8	1.9491e-004	1.9820e-004
	F20GF17.6	1.3458e-004	1.3650e-004
	F20GF25.4	1.0910e-004	1.1119e-004
	F20GF35.3	9.0669e-005	9.0983e-005

Table No.13: Deflection of clamped edge glass fibers reinforced Resol/VAC-EHA Composite plate

q = 10 (N/m^2), a = b = 300 (mm) h = 10 (mm)	Sample Code	Analytical Method w_{max} [22] (mm)	MQRBF Method w_{max} (mm)
	Resol	3.2211e-004	3.2452e-004
	F5	3.4292e-004	3.4549e-004
	F10	3.4719e-004	3.4980e-004
	F15	3.5158e-004	3.5421e-004
	F20	3.6541e-004	3.6819e-004